Sequential roles for myosin-X in BMP6-dependent filopodial extension, migration, and activation of BMP receptors

Xinchun Pi,[1] Rongqin Ren,[1] Russell Kelley,[1] Chunlian Zhang,[1] Martin Moser,[4] Aparna B. Bohil,[2] Melinda DiVito,[2] Richard E. Cheney,[1,2] and Cam Patterson[1,3]

[1]Carolina Cardiovascular Biology Center, [2]Department of Cell and Molecular Physiology, and [3]Department of Medicine, University of North Carolina, Chapel Hill, NC 27599
[4]Innere Medizin III, Universität Freiburg, 79106 Freiburg, Germany

Endothelial cell migration is an important step during angiogenesis, and its dysregulation contributes to aberrant neovascularization. The bone morphogenetic proteins (BMPs) are potent stimulators of cell migration and angiogenesis. Using microarray analyses, we find that myosin-X (Myo10) is a BMP target gene. In endothelial cells, BMP6-induced Myo10 localizes in filopodia, and BMP-dependent filopodial assembly decreases when Myo10 expression is reduced. Likewise, cellular alignment and directional migration induced by BMP6 are Myo10 dependent. Surprisingly, we find that Myo10 and BMP6 receptor ALK6 colocalize in a BMP6-dependent fashion. ALK6 translocates into filopodia after BMP6 stimulation, and both ALK6 and Myo10 possess intrafilopodial motility. Additionally, Myo10 is required for BMP6-dependent Smad activation, indicating that in addition to its function in filopodial assembly, Myo10 also participates in a requisite amplification loop for BMP signaling. Our data indicate that Myo10 is required to guide endothelial migration toward BMP6 gradients via the regulation of filopodial function and amplification of BMP signals.

Introduction

The bone morphogenetic proteins (BMPs) play important roles in cellular processes such as proliferation, differentiation, motility, adhesion, cell death, and the specification of cell fate during embryogenesis (Hogan, 1996; Zhang and Bradley, 1996; Massague, 1998; Wozney, 2002). Both in vitro and in vivo assays indicate that assembly of new blood vessels via vasculogenesis and angiogenesis depends on BMP signaling via direct effects on endothelial cells (Yamashita et al., 1997; Moutsatsos et al., 2001; Valdimarsdottir et al., 2002). For example, BMP2 stimulates endothelial proliferation, migration, and tube formation during tumor neovascularization (Raida et al., 2005), and our laboratory recently reported that BMP6 enhances in vitro angiogenesis via cyclooxygenase 2–dependent prostanoid generation (Ren et al., 2007). Similarly, mice null for Smad5, a transcriptional activator of BMP responses, die between days 10.5 and 11.5 of gestation as a result of defective vascular development typified by abnormal vasculature and irregularly distributed blood cells in the yolk sac (Yang et al., 1999). Collectively, these data support a model in which BMPs critically regulate angiogenesis and embryonic development under diverse circumstances.

There are two mechanistically distinct types of angiogenesis: sprouting angiogenesis and nonsprouting angiogenesis (also called intussusception; Folkman and Klagsbrun, 1987; Klagsbrun and D'Amore, 1991; Patan et al., 1996). Intussusception occurs by the proliferation of endothelial cells within a vessel and the formation of a large lumen that splits by the insertion of tissue columns into vessels (Patan, 2000). In the case of sprouting angiogenesis, migration of existing endothelial cells is critical for new vessel formation. In angiogenic extensions in the brain, endothelial cells at the tip of the sprout develop filiform processes (Klosovskii and Zhukova, 1963). There is evidence from previous studies that endothelial sprouts can extend multiple filopodia at their distal tips (Bar and Wolff, 1972; Marin-Padilla, 1985), indicating that growing vascular sprouts are endowed with specialized tip structures with potential functions in guidance and migration. Filopodia and related structures such as microspikes, cytonemes, and microvilli are thin

Correspondence to Cam Patterson: cpatters@med.unc.edu

Abbreviations used in this paper: BMP, bone morphogenetic protein; MEC, mouse intraembryonic endothelial cell; SEM, scanning EM.

The online version of this article contains supplemental material.

The Journal of Cell Biology, Vol. 179, No. 7, December 31, 2007 1569–1582
http://www.jcb.org/cgi/doi/10.1083/jcb.200704010

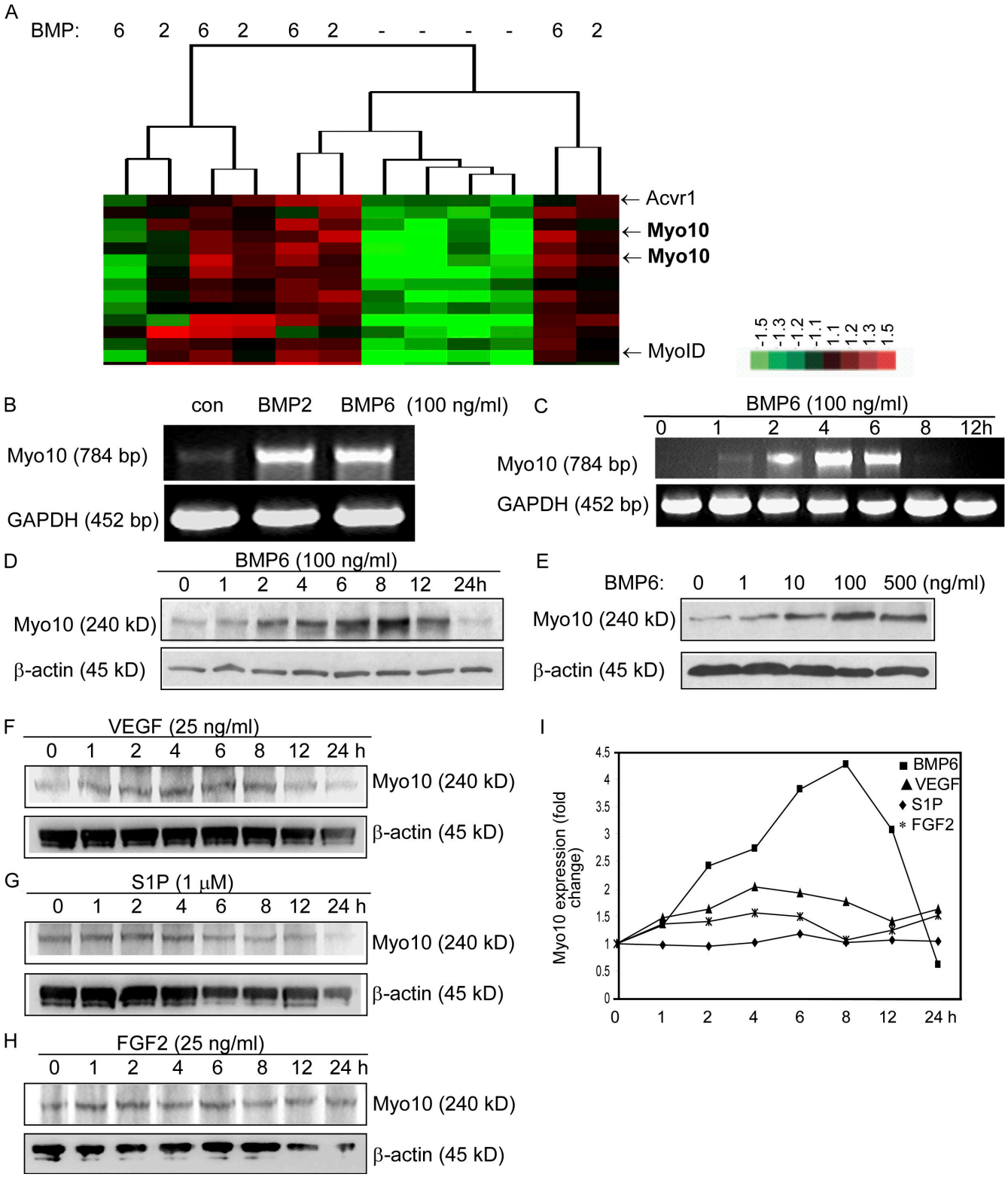

Figure 1. **Myo10 is up-regulated by BMP2 and BMP6 treatment.** (A) Microarray analysis was performed with RNA samples purified from MECs treated with BMP2, BMP6, or DMSO for 4 h (Ren et al., 2007). Differentially expressed genes were selected with a p-value ≤0.05 and ratio fold change ≥±1.5 and were subjected to hierarchical cluster analysis. Median-centered clusters were viewed with JavaTreeView. Fold change relative to common reference is indicated by red (+1.5; full scale) and green (−1.5; full scale) intensity. This image is a group of clustered genes with selected genes labeled. (B) MECs were treated with BMP2 and BMP6, and the total RNA was used for RT-PCR analysis with Myo10-specific primers. Glyceraldehyde-3-phosphate dehydrogenase (GAPDH) was used as an internal control. (C) RT-PCR analysis of Myo10 transcripts after BMP6 treatment for the indicated times. (D) Western blotting analysis of Myo10 protein expression after BMP6 treatment for the indicated times. (E) Western blotting analysis of Myo10 protein expression after BMP6 treatment for 8 h with the indicated dosages. (F–I) Myo10 is up-regulated by BMP6 and VEGF but not by S1P and FGF-2 treatment. (F–H) MECs were treated with VEGF (F), S1P (G), and FGF2 (H) for the indicated times. The cell lysates were subjected to Western blotting analysis of Myo10 protein

cylindrical extensions of the cell membrane that are filled with long actin filaments organized as a tight bundle with their barbed ends (fast growing ends) pointing toward the direction of protrusion (Small, 1988). Filopodia are used by many cell types as sensing organs to explore the extracellular matrix and surface of other cells. However, the role of filopodia in directed endothelial migration and sprouting angiogenesis is still a mystery and receives little notice in today's concepts of vascular development.

Because the mechanisms by which BMPs induce angiogenesis are still poorly understood and the molecular players responsible for the initiation of endothelial migration and subsequent new blood vessel formation are not clear, we performed gene expression profile analysis of the BMP6-mediated signaling network in endothelial cells. Myosin-X (Myo10), an unconventional myosin critical for filopodial formation (Bohil et al., 2006), was induced by BMP2 and BMP6 in these studies. Specialized filopodia known as cytonemes in *Drosophila melanogaster* orient along a decapentaplegic (orthologue of BMP) gradient (Hsiung et al., 2005), and long filopodia extending from tip endothelial cells under the guidance of VEGF-A are required for early postnatal retina vasculature formation (Gerhardt et al., 2003). Because of this, we hypothesized that BMPs might stimulate filopodial formation and directed migration in endothelial cells and that up-regulation of Myo10 is a critical cue for the endothelium when probing the local environment during blood vessel assembly is required.

Results

Identification of Myo10 as a BMP target gene in endothelial cells

To better understand the mechanistic roles of BMPs in angiogenesis, we identified candidate BMP-responsive genes in endothelial cells using microarray technology. Total RNA samples were extracted from mouse intraembryonic endothelial cells (MECs) untreated or treated with BMP2 or BMP6 for 4 h. Among the regulated genes, Myo10 was up-regulated in cells treated with either BMP2 or BMP6 (Fig. 1 A). The up-regulation of Myo10 by BMP2 and BMP6 was confirmed at both the mRNA and protein levels. RT-PCR analysis indicated that Myo10 RNA levels increased dramatically after 100 ng/ml BMP2 or BMP6 treatment for 4 h in MECs (Fig. 1 B). Peak induction of Myo10 after BMP6 treatment occurred at 4 h for Myo10 mRNA and at 8 h for Myo10 protein (Fig. 1, C and D). The induction of Myo10 protein by BMP6 occurred in a dose-dependent fashion (Fig. 1 E). A similar increase in Myo10 protein level was also detected in human endothelial cells treated with BMP6 (unpublished data). Based on these results, 8-h treatment of 100 ng/ml BMP6 was used in the following experiments unless otherwise stated. To determine whether Myo10 could also be induced by other angiogenic factors, we stimulated MECs with VEGF, sphingosine-1–phosphate (S1P), and FGF-2. None of these factors were able to induce the level of Myo10 production seen with BMP6 stimulation; there was a modest increase in Myo10 protein levels associated with VEGF treatment (Fig. 1 F) but almost no change seen with either S1P or FGF-2 (Fig. 1, G and H). This comparison of BMP6 to other angiogenic factors (Fig. 1 I) supports the hypothesis that Myo10 is a relatively BMP-specific target gene.

Using immunofluorescence staining, we found that BMP6 treatment qualitatively increased the number of filopodial extensions in MECs (Fig. 2; compare G–I with the untreated cells in D–F). In addition, BMP6 stimulation induced the localization of Myo10 into filopodial projections of MECs (Fig. 2, compare H with E). The staining of Myo10 in the cytoplasm of BMP6-treated cells (Fig. 2 H) indicated the expression of Myo10 in the cytosol compartment, which might represent the protein pool of Myo10 available for translocation into filopodia when filopodial assembly is needed. The images stained with control IgG (Fig. 2 B) demonstrated the specificity of the anti-Myo10 polyclonal antibody. In addition, we found that overexpressed GFP-tagged Myo10 protein in MECs induced marked changes in MEC morphology (including a dramatic increase in the number of filopodia) even in the absence of BMP6 stimulation, and GFP-Myo10 specifically localized within filopodial extensions (Fig. 2 K). These data indicate that BMP6 stimulation induces filopodial extensions into which Myo10 localizes and that increased expression of Myo10 alone is able to direct filopodial assembly in the absence of external cues. These observations suggested a fundamental role for Myo10 in the mechanistic events that are required for BMP-dependent vessel formation and prompted us to explore this relationship further.

Requirement of Myo10 for BMP6-dependent filopodial assembly

To test the functional role of Myo10 in MECs, we knocked down the expression of endogenous Myo10 by siRNA generated with a plasmid system that also coexpressed GFP from a second locus within the vector so that transfection could be monitored at the single-cell level. Among the four different siRNAs tested, Myo10-siRNA1 and Myo10-siRNA2 significantly decreased Myo10 protein levels (Fig. 3 A). Given that our transfection efficiency of MECs was ~40%, we surmise that Myo10 mRNA was suppressed by ≥80% by these siRNAs after BMP6 stimulation. Immunofluorescence analyses further confirmed that Myo10 siRNA1 and Myo10 siRNA2 efficiently knocked down Myo10 expression induced by BMP6 in transfected cells compared with untransfected cells or control siRNA-transfected cells (unpublished data).

To quantitatively assess the effects of BMP6 on filopodial extension and the role of endogenous Myo10 in this process, high resolution imaging with correlative fluorescent scanning EM (SEM) was performed (Bohil et al., 2006). MECs transfected

expression and actin as the internal control. (I) Comparison of Myo10 expression level after BMP6, VEGF, S1P, and FGF-2 treatment. The band intensity was measured and quantitated by ImageJ.

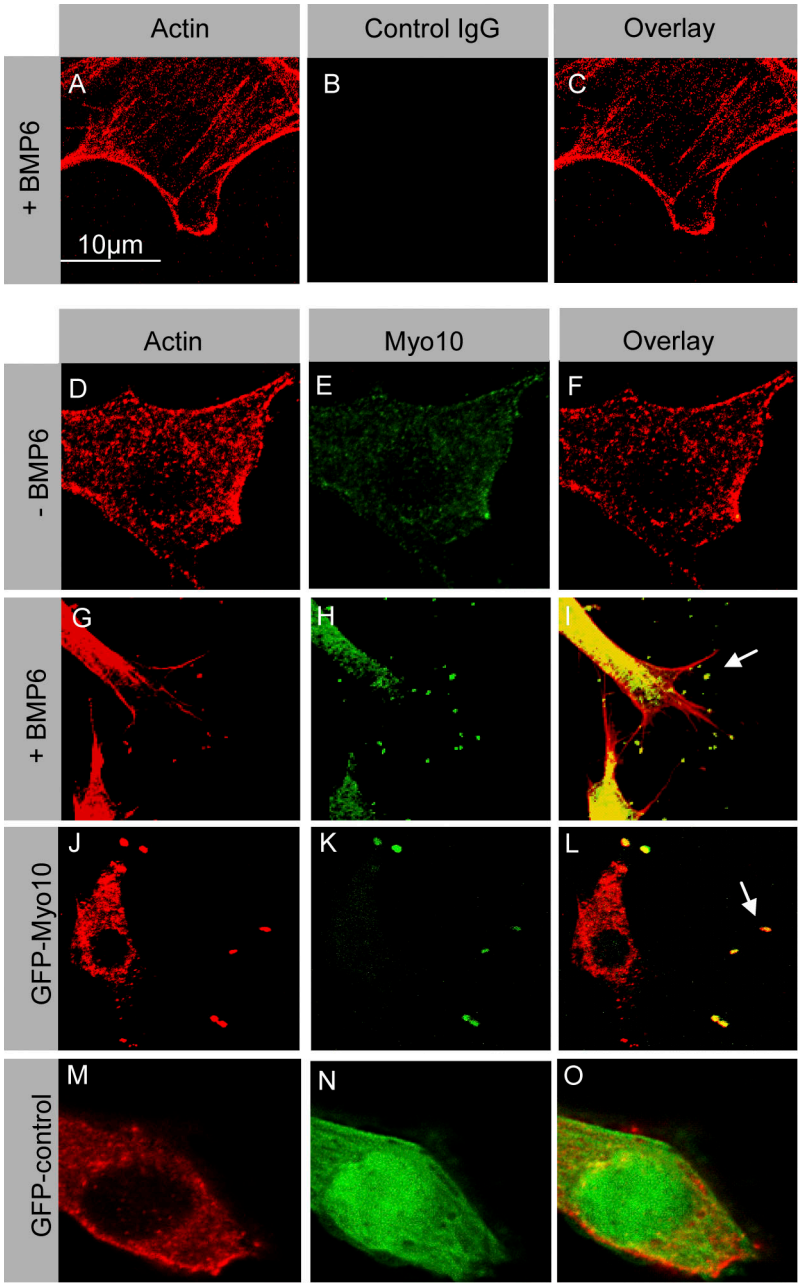

Figure 2. **Myo10 induced by BMP6 is localized in filopodia.** MECs were treated with BMP6 for 8 h (A–C and G–I) or DMSO (D–F) and were fixed with PFA. Cells were stained with phalloidin (A, D, G, J, and M) and chicken anti–mouse Myo10 pAb (E and H) or control IgG (B) as a negative control. Exogenous Myo10 (GFP tagged) was expressed by transiently transfecting MECs with a plasmid encoding GFP-Myo10 (J–L). GFP control plasmids (M–O) were transfected in MECs as the negative controls for GFP-Myo10. Actin was visualized using Texas red–phalloidin (red). Myo10 was visualized using chicken anti-Myo10 pAb (green; E and H) or GFP (green; K and N). The arrows represent filopodia.

with GFP-expressing Myo10 siRNA plasmids were cultured on etched grid coverslips to localize the transfected cells. The cells were then treated with BMP6 for 8 h and processed for SEM imaging (Fig. 3, B–H). BMP6 treatment increased filopodial number on the cell surface (from 14 ± 9 to 59 ± 17). The majority of BMP6-induced filopodia were substrate-attached filopodia (Fig. 3 E); thus, we tested whether or not there was a substrate-specific effect of filopodial formation or attachment by growing cells on collagen- and fibronectin-coated dishes. No difference was seen between the different substrates, (unpublished data) and so, for the remainder of our experiments, we used collagen as the adhesion factor unless otherwise stated. Formation of filopodia after BMP6 stimulation was almost completely suppressed by Myo10 siRNA1 and Myo10 siRNA2 (from 59 ± 17 to 19 ± 9 or 20 ± 10; Fig. 3, F and G). It has been shown previously that Myo10 can stimulate the assembly of filopodial processes (Bohil et al., 2006), although the precise physiologic context for these events has not been clear. These data support a requisite physiological role for Myo10 in filopodial formation induced by BMP6 in endothelial cells. BMP6 increased filopodia number in endothelial cells (Fig. 3, B–H) but did not further enhance the filopodial formation induced by the overexpression of Myo10 (not depicted). It was previously suggested that Myo10 functions downstream of Cdc42 for formation of the filopodial extensions. In the study performed by Bohil et al. (2006), Myo10 siRNA inhibited the filopodial extensions increased by constitutively active Cdc42, but dominant-negative Cdc42 did not inhibit filopodia formation induced by Myo10 overexpression. However, when we performed Cdc42 and Rac1 activity assays, we found that their activities were not increased by BMP6 treatment in endothelial

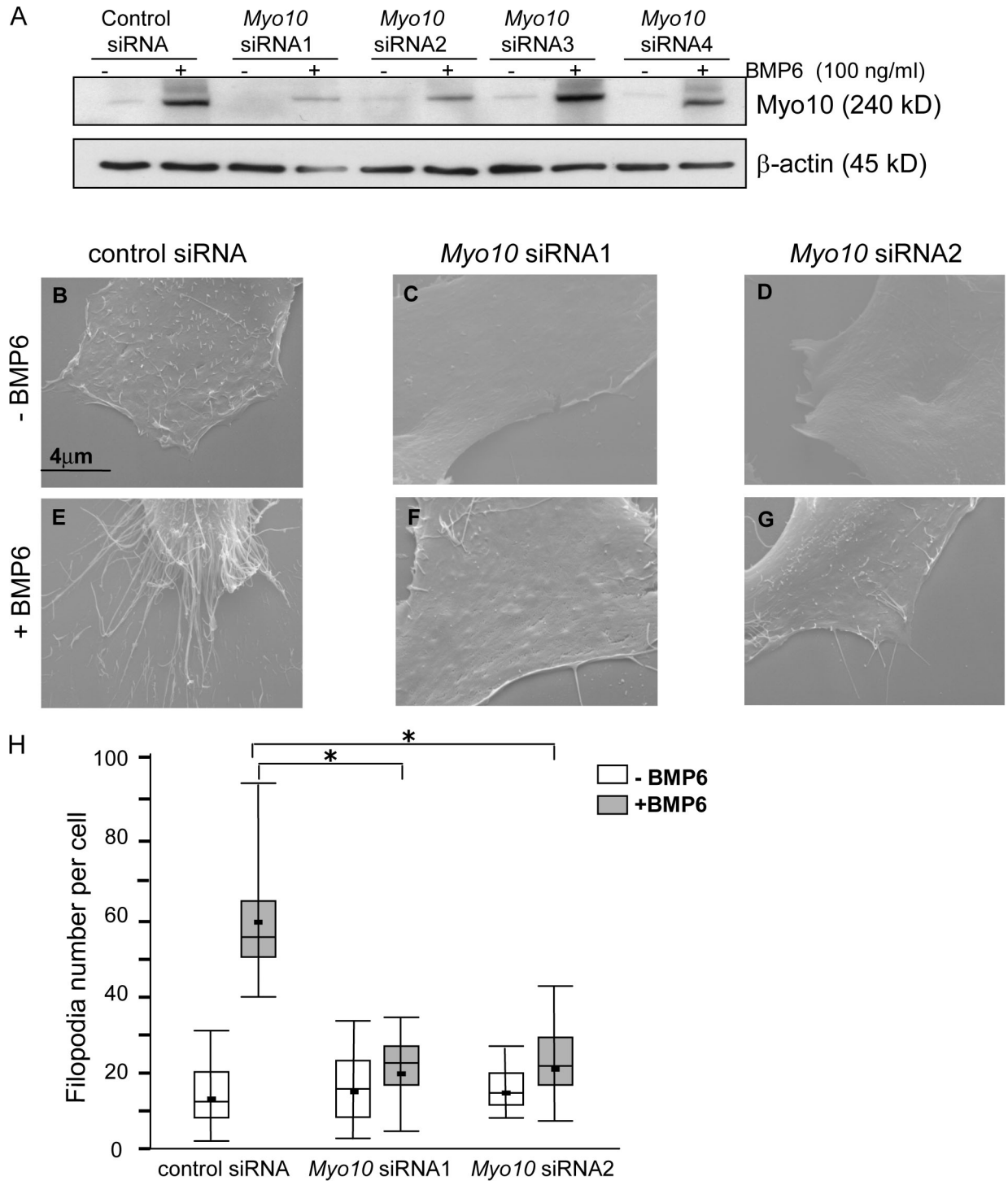

Figure 3. **Myo10 siRNAs inhibit BMP6-induced filopodia.** (A) MECs transfected with Myo10 siRNAs were lysed and subjected to Western blotting analysis with anti-Myo10 pAb (top). A β-actin blot of the same membrane controlled for sample loadings (bottom). (B–H) Knockdown of endogenous Myo10 in MECs by Myo10 siRNAs decreased filopodial number in the BMP6-treated conditions. MECs were transfected with GFP-tagged Myo10 siRNA1 (C and F) or siRNA2 (D and G) or by the GFP-tagged control vector containing irrelevant siRNA sequence (B and E). Cells were treated with 100 ng/ml BMP6 (E–G) or DMSO (B–D) as a control, and GFP-positive cells were subjected for SEM analysis. (H) The bar graphs show quantification of filopodial numbers in MECs transfected with GFP-tagged control siRNA, GFP-Myo10 siRNA1, or GFP-Myo10 siRNA2. *, $P < 0.05$; $n = 3$. $n = 20$ cells per sample.

cells (unpublished data), suggesting that the basal activity of Cdc42 in endothelial cells might be strong enough to permit Myo10-mediated filopodial formation induced by BMP6 and that the effects of BMP6 are not directly mediated through the activation of Cdc42.

Myo10 is critical for cell alignment toward a BMP gradient

To further test whether Myo10-dependent filopodia act as sensors in the directed cell movement regulated by BMP6, we used Dunn chamber assays. In these assays, a radially directed linear

diffusion gradient is established within 10–30 min that has a half-life of 10–30 h (Zicha et al., 1991). For our studies, MECs cultured on coverslips were pretreated with BMP6 for 4 h to induce the expression of Myo10 and filopodia and were cultured in the Dunn chamber for another 4 h to establish a directed BMP6 gradient. Cells were stained to identify nuclei (with DAPI) in combination with a Golgi marker (GM130) and filamentous actin (phalloidin), which revealed the cell polarity and orientation of migration. Without BMP6 pretreatment or BMP6 gradient media, cells did not align toward any direction (Fig. 4 A). After either BMP6 pretreatment or establishment of a BMP6 gradient, cells polarized but failed to align toward the BMP6 gradient (Fig. 4, B and C). With BMP6 pretreatment plus culturing under conditions to establish a subsequent BMP6 gradient, cells unanimously aligned toward the BMP6 gradient (Fig. 4 D). These experiments indicate that both BMP6 pretreatment and the presence of a BMP6 gradient are necessary for cell reorientation toward the gradient.

To determine whether induction of Myo10 by BMP6 during the pretreatment period is required for directed cell polarization, we knocked down Myo10 expression with Myo10 siRNA (Fig. 4, E–K). MECs transfected with control siRNA and pretreated with BMP6 for 4 h before application of the BMP6 gradient demonstrated increased alignment toward the BMP6 gradient (from 32 ± 10 to 95 ± 5%; Fig. 4 E). However, cells transfected with Myo10 siRNA1 under the same conditions demonstrated perturbed Golgi reorientation after the pretreatment of BMP6 compared with similarly transfected cells without BMP6 pretreatment (from 32 ± 10 to 35 ± 8%; Fig. 4 F). Similarly, MECs expressing Myo10 siRNA2 also failed to align in the proper direction (from 28 ± 7 to 27 ± 9%; Fig. 4 G). These knockdown cells (Fig. 4, F and G; arrowheads; and expressing GFP in I and J) are well controlled for by the nontransfected cells in the same images that do not express GFP, which still successfully reorient toward the BMP6 gradient. These data strongly support a model in which Myo10 expression and consequent filopodial assembly are required for endothelial cells to sense and respond to the guidance cue BMP6.

Role of Myo10 in BMP6-dependent directed migration of endothelial cells

To extend our observations, we performed assays to determine the importance of Myo10-dependent filopodia formation in directed cell migration. Wound healing assays of MECs demonstrated that BMP6 increased cell migration toward the wound area from 52.4 ± 6.5 to 81.3 ± 8.2% (Fig. 5 A). Myo10 induced by BMP6 was localized to the tip of filopodia in endothelial cells on the leading edge of the wound compared with the cells without BMP6 treatment, as shown by immunofluorescence microscopy (Fig. 5, B and D). SEM images also demonstrated that more filopodia formed on endothelial cells at the leading edge of the migration front after BMP6 treatment compared with control (Fig. 5, C and E).

To specifically test the role of Myo10 in directed migration, we performed Boyden chamber assays to determine whether BMP-dependent directional migration is inhibited by Myo10 knockdown with siRNA (Fig. 5 F). MECs were transfected with Myo10 siRNA1, Myo10 siRNA2, or control siRNA as indicated. Cells were then pretreated with BMP6 for 4 h and placed into Boyden chambers in the presence of a BMP6 gradient. BMP6 pretreatment significantly increased directed cell migration induced by the BMP6 gradient from 7 ± 2 to 52 ± 10 cells compared with cells without BMP6 pretreatment (from 7 ± 2 to 18 ± 14 cells). This increase in migration was inhibited by Myo10 knockdown with Myo10 siRNA1 (from 52 ± 10 to 4 ± 2 cells) or Myo10 siRNA2 (from 52 ± 10 to 3 ± 5 cells), which indicates that Myo10-mediated filopodial formation induced by BMP6 pretreatment is critical for BMP6-guided endothelial cell migration. Other angiogenic factors (VEGF, FGF-2, and S1P) were also able to induce directed cell migration; however, only the VEGF-induced migration was inhibited by disruption of filopodia with Myo10 siRNA2 (Fig. S1, available at http://www.jcb.org/cgi/content/full/jcb.200704010/DC1). The combined treatment of BMP6 and VEGF produced a small but not additive increase in migration compared with that seen with either drug on its own, suggesting that BMP6 and VEGF do not work synergistically with each other.

Without a BMP6 gradient, cells pretreated with BMP6 also increased their migration in this assay, albeit to a lesser extent (from 7 ± 2 to 34 ± 9 cells). This suggested to us that increased filopodia formation induced by BMP6 pretreatment also increased random cell migration in this assay even though cell reorientation fails to occur under these conditions. To test this hypothesis directly, we performed a random cell migration analysis using a live image recording system to monitor the speed and distance of cellular migration. BMP6 treatment increased the speed of endothelial cell migration from 0.060 ± 0.016 to 0.146 ± 0.032 μm/min (Fig. S2 and Table S1). This effect was Myo10 dependent, as treatment of cells with Myo10 siRNA2 decreased the speed of random migration to near control levels (0.070 ± 0.020 μm/min).

Role of Myo10 in BMP6-dependent tube formation

Endothelial cell migration is a critical step for tube formation during angiogenesis. To test the importance of Myo10 and filopodia in higher order cell assembly processes, we examined the effect of Myo10 on the formation of capillary-like tubes formed in matrigel (Ren et al., 2007). MECs were transfected with Myo10 siRNA1, Myo10 siRNA2, or control siRNA. The next day, cells were serum starved for 1 h and plated on matrigel in medium containing 100 ng/ml BMP6. Treatment with BMP6 significantly stimulated capillary-like structure formation at 6 h compared with cells without treatment (unpublished data): the cord length increased from 237 ± 41 to 783 ± 231 μm. In the Myo10 siRNA1–expressing cells, capillary-like structure formation was inhibited by ∼60.9%. Similarly, capillary-like structure formation was inhibited by ∼53.9% in Myo10 siRNA2–expressing cells. To exclude the possibility that the observed tube formation was merely a result of the matrigel environment in which the cells were plated, we performed a 3D collagen angiogenesis assay and verified that tubulogenesis did occur when endothelial cells were treated for extended periods of time with BMP6 (Fig. 5 J and Fig. S3, available at http://www.jcb.org/cgi/ content/full/jcb.200704010/DC1) compared with cells without treatment

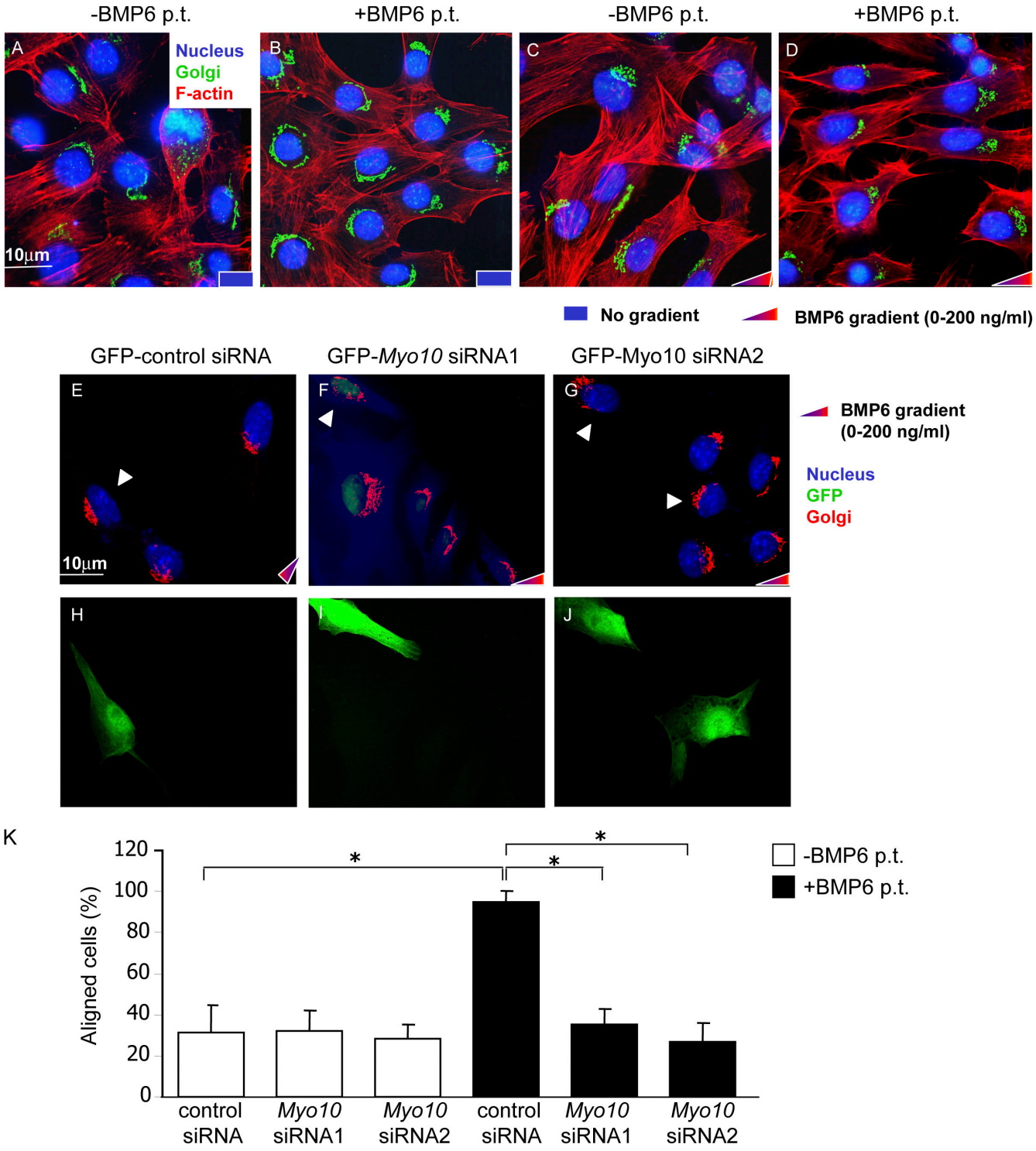

Figure 4. **Cell alignment is dependent on Myo10.** (A–D) MECs aligned toward the BMP6 gradient. Cells cultured on the coverslips were pretreated with BMP6 (B and D) or DMSO (A and C) for 4 h, were transferred to the Dunn chamber with the media containing 0–200 ng/ml BMP6 gradient (C and D) or not containing gradient (A and B), and were maintained for 4 h. Cells were fixed and stained with phalloidin, DAPI, and GM130. Actin (Texas red–phalloidin), red; Golgi (anti-GM130 mAb), green; nucleus (DAPI), blue. (E–K) Knockdown of endogenous Myo10 in MECs by Myo10 siRNAs inhibited cell alignment. (E–J) Cells were transfected with GFP-Myo10 siRNA1 or GFP-Myo10 siRNA2 and controlled by transfecting cells with GFP-tagged control vector containing irrelevant siRNA sequence. The cells were pretreated with BMP6 for 4 h and were transferred into the Dunn chamber for another 4 h with 0–200 ng/ml of the media containing BMP6 gradient. The cells were fixed, and immunofluorescent images were taken. GFP, green; Golgi (anti-GM130 mAb), red; nucleus (DAPI), blue. White arrowheads represent the transfected cells with siRNAs (GFP positive). (K) Quantitative analysis of the aligned cells toward the higher BMP6 gradient. Error bars represent SD. $n = 3$; *, $P < 0.05$. n = at least 57 cells per sample. p.t., pretreatment.

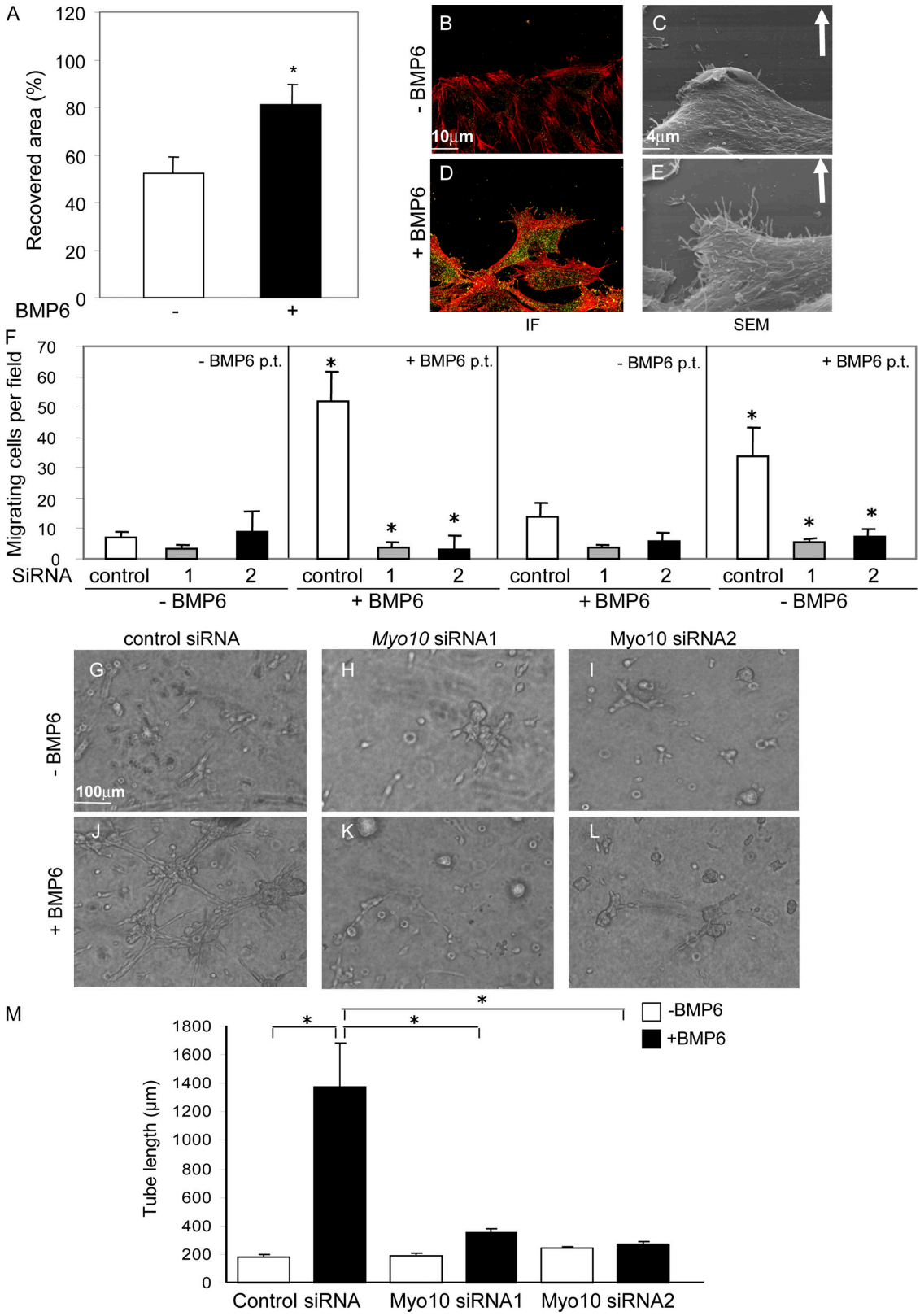

Figure 5. **Myo10 knockdown inhibits directed cell migration and angiogenesis induced by BMP6.** (A–E) BMP6 increased Myo10 proteins in filopodia, filopodial number, and directed migration. Wound-healing assay was performed with MECs grown on 35-mm wells. (A) The bar graph shows the recovered area after cells were stimulated with BMP6 for 16 h. (B and D) The immunofluorescent staining of cells. Actin (Texas red–phalloidin), red; Myo10 (anti-Myo10 pAb), green; overlay of the red and green, yellow. The increased yellow staining demonstrated the increased localization of Myo10 protein at the filopodial tips of the cells on the leading edge, where the filopodial number also increased. (C and E) The increase of filopodial number in SEM images of cells. Arrows represent the migration direction of the cells. IF, immunofluorescence; SEM, scanning EM. (F) Myo10 knockdown inhibited directed cell migration induced by BMP6. MECs were transfected with GFP-Myo10 siRNA1, GFP-Myo10 siRNA2, or control siRNA, were pretreated with BMP6 for 4 h, and

(Fig. 5 G). Tube formation was inhibited by 80.2% and 93.1% in the Myo10 siRNA1– and Myo10 siRNA2–expressing cells, respectively (Fig. 5, H, I, K, and L). Quantitative data are presented in Fig. 5 M. These data strongly indicate that Myo10 and filopodia are critical factors in endothelial cell migration and angiogenesis.

Association of Myo10 with the BMP receptor ALK6

The preceding experiments indicate that induction of Myo10 by BMP6 is required for BMP6-dependent filopodial assembly, which, in turn, is required for endothelial cells to respond in a directed fashion to BMP6 gradients. This suggested to us that Myo10 might have additional roles in regulating BMP6 signaling responses beyond its necessary role in inducing filopodial processes on BMP-stimulated endothelial cells. Like most myosins, the Myo10 heavy chain can be divided into three parts: head, neck, and tail. The head domain contains the motor activity. There are three IQ motifs in the neck region that are predicted to associate with calmodulin or a calmodulin-like light chain. The tail domain contains a coiled-coil domain, a PEST region, three pleckstrin homology domains, an MyTH4 domain, and a FERM domain (Sousa and Cheney, 2005). An interaction between the Myo10 FERM domain and an NPXY motif within β-integrin cytoplasmic domains regulates integrin relocalization and the formation of substrate-attached filopodia (Zhang et al., 2004). To explore the possibility that Myo10 modulates BMP6 signaling, we examined the localization of the BMP6 receptor ALK6 (expressed as a GFP fusion) in MECs stimulated with BMP6. Under these conditions, a fraction of ALK6 was localized in filopodia (Fig. 6 A). The ALK6-containing puncta moved from cytoplasm to filopodia and possessed intrafilopodial motility (Fig. 6 and Video 1, available at http://www.jcb.org/cgi/content/full/jcb.200704010/DC1). The mean rate of the forward movements was $\sim 42 \pm 16$ nm s^{-1} ($n = 10$ puncta). When coexpressed, ALK6 (tagged with HA) and GFP-Myo10 colocalized in the tips of filopodia of BMP6-stimulated MECs (Fig. 6 B).

Based on this temporal and spatial colocalization, we tested the possibility of association between Myo10 and ALK6 by coimmunoprecipitation. Overexpressed HA-ALK6 efficiently coimmunoprecipitated with GFP-Myo10 in 293T cells (Fig. 6 C), as did endogenous ALK6 and Myo10 in MECs (Fig. 6 D). Using time-lapse video microscopy, we observed the cotransportation of Myo10 and ALK6, providing additional support that Myo10 and ALK6 move together within the filopodia under certain circumstances (Video 2). However, we also observed some infrequent instances within filopodia in which these two molecules appeared to move independently of each other, suggesting that either the amount of Myo10 cotransporting with ALK6 is below the detection limits under some circumstances or that there are other unknown Myo10-independent mechanisms for ALK6 transportation. In any event, these data support a model in which Myo10 binds to and is required for the transport of ALK6 to filopodia, indicating that the association between Myo10 and ALK6 likely plays important roles in coordinating filopodial function and BMP signaling during directed endothelial cell migration and angiogenesis.

Myo10 is required for optimal intracellular responses to BMP stimulation in endothelial cells

We observed that Myo10 was not only required for BMP6-dependent filopodial assembly and consequent directed migration and angiogenesis of endothelial cells but also that the BMP receptor ALK6 was associated with Myo10 in filopodia. This suggested to us that Myo10 not only responds to BMP stimulation but might also be required for maximal BMP signal generation. It is known that BMPs transduce signals through trans-membrane serine-threonine kinase receptors, including type I and II receptors. Upon BMP-induced heteromeric complex formation, the constitutively active serine/threonine kinse of the type II receptor phosphorylates type I receptor on its GS domain. The activated type I receptor phosphorylates regulatory Smads (Smad1, 5, and 8). This phosphorylation of Smads by type I receptor is inhibited by inhibitory Smads (Smad6 and 7). The association of regulatory Smads with common partner Smads (Smad4) leads to the translocation of heteromeric Smads to the nucleus and the activation of transcriptional machinery for BMP-responsive genes (ten Dijke et al., 2003). To test the involvement of Myo10 in BMP6-transduced intracellular signaling events, we used Myo10 siRNA to knock down Myo10 protein to inhibit filopodial assembly and the association between ALK6 and Myo10. In control cells, we observed that the major signaling downstream of BMP6 receptor ALK6 activation (specifically, Smad1, 5, and 8 phosphorylation) was induced by BMP6 after 30 min of treatment and lasted for at least 8 h. Myo10 knockdown with Myo10 siRNA2 significantly inhibited the activation of Smads (Fig. 7). These experiments indicate that Myo10 is not only critical for filopodial assembly but is also required for BMP6 receptor–mediated endothelial activation by amplifying BMP responses, which mechanistically explains the important role of Myo10 in BMP6-induced directed migration of endothelial cells and angiogenesis.

Discussion

The major observation of this study is that Myo10 is critically important in a filopodial sensor mechanism that mediates BMP6-guided endothelial cell migration and angiogenesis. Specifically, BMP6 potently induces Myo10 expression, and Myo10, in turn, is required for filopodial formation, cell alignment, directed migration, and tube formation induced by BMP6. Additionally,

were trypsinized for the Boyden chamber assay. The cells migrating through the filter were counted. p.t., pretreatment. (G–M) Myo10 knockdown inhibited tube formation induced by BMP6 using 3D collagen assay. MECs were transfected with GFP-Myo10 siRNA1, GFP-Myo10 siRNA2, or control siRNA and were lysed for the 3D collagen angiogenesis assay. (G–L) The brightfield images were taken after 24 h of incubation. (M) Quantitation of the tube formation. Error bars represent SD. $n = 3$; *, $P < 0.05$.

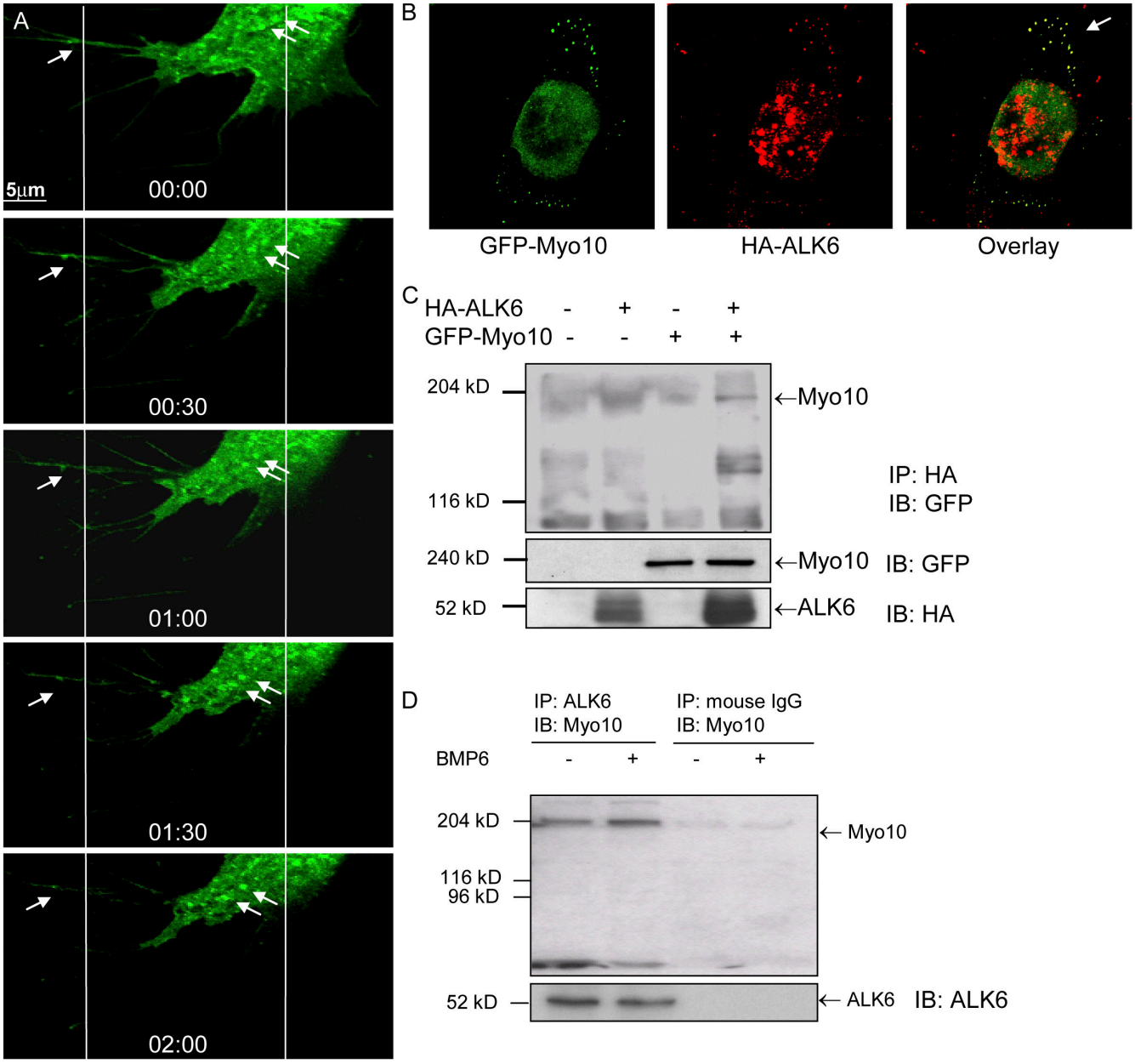

Figure 6. **Myo10 interacts with ALK6.** (A) Selected sequence from a time-lapse video focusing on the movements of puncta containing GFP-ALK6 proteins. Arrows represent the puncta containing GFP-ALK6. The images were taken every 30 s for 120 s after MECs were treated with BMP6 for 4 h. The mean rate of the forward movements for the puncta was ~42 ± 16 nm s^{-1} (n = 10 puncta). (B) Colocalization of exogenous GFP-tagged Myo10 and HA-tagged ALK6 at tips of filopodia in HeLa cells. Myo10 (GFP), green; ALK6 (anti-HA mAb), red. The arrow indicates colocalization. (C) Exogenous Myo10 associated with exogenous ALK6. GFP-Myo10 and HA-ALK6 were expressed in 293T cells, and immunoprecipitation was performed with anti-HA mAb followed by Western blotting against GFP. (D) Endogenous Myo10 associated with ALK6. MEC lysates were immunoprecipitated by anti-ALK6 mAb, with mouse IgG as a control, followed by Western blotting against Myo10.

Myo10 associates with the BMP6 receptor ALK6 and modulates BMP6-dependent endothelial activation by regulating the phosphorylation of Smads, the direct downstream transcriptional targets of the BMP receptors. These experiments extend the previous observation that Myo10 induces nondirectional filopodial formation (Bohil et al., 2006) and indicate that Myo10 serves as a critical integration node in growth factor signaling to facilitate directional probing of the local cellular environment as well as further amplification of growth factor signaling that is relevant to the pathophysiologically critical process of angiogenesis.

There is increasing evidence that secreted signaling molecules within the BMP subfamily of the TGFβ superfamily are key regulators in the morphogenesis of multiple organ systems, including angiogenesis. VEGF and Id1 were among only a small number of identified downstream targets of BMPs responsible for vascular development and angiogenesis (Deckers et al., 2002; Valdimarsdottir et al., 2002) that was expanded by experiments from our laboratory that identified multiple transcriptional targets of BMP2 and BMP6 in endothelium using microarray technology (Ren et al., 2007). A necessary role for

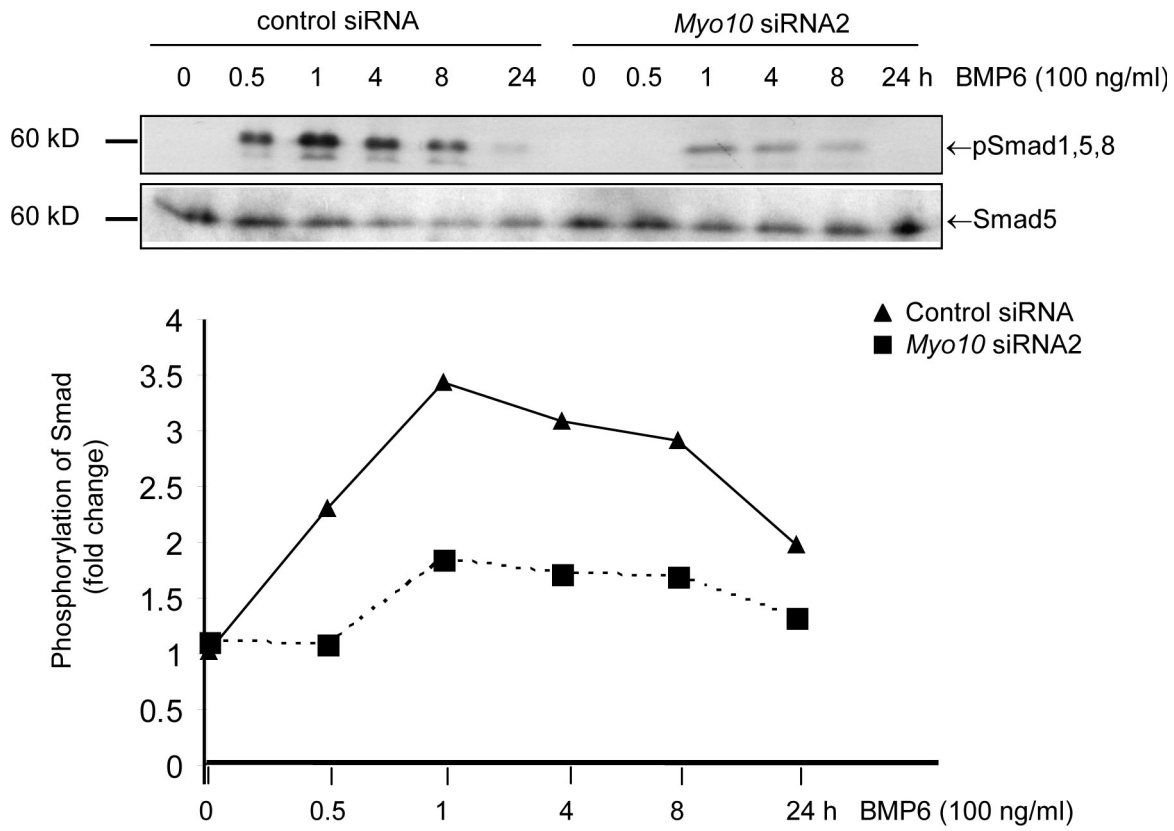

Figure 7 . **Myo10 knockdown inhibits BMP6-induced Smad1, 5, and 8 activation.** MECs were transfected with Myo10 siRNA2 or control siRNA and were stimulated with BMP6 for the indicated times for the activation of Smads. Cells were lysed for Western blotting analysis of the antiphospho-Smad1, 5, and 8 pAb, anti-Smad5 pAb, and anti-Myo10 pAb. This is a representative image of three independent experiments.

cyclooxygenase 2–dependent prostanoid generation was identified for BMP6-induced angiogenic responses through these inductive experiments (Ren et al., 2007). The identification of Myo10 as a BMP6-responsive gene expands the list of bona fide BMP targets in endothelium and begins to paint a picture of a coordinated program in which growth factors, intracellular signaling pathways, and active structural processes are coordinated by BMPs to create new blood vessels.

Filopodia are best characterized in growth cones of migrating axons that sample the external environment, searching for guidance cues that allow the growing axon to navigate over long distances and find appropriate targets (Tessier-Lavigne and Goodman, 1996). This study is the first to provide direct evidence indicating the physiological importance of Myo10 and filopodia as sensors in directed endothelial migration and angiogenesis. Myo10 is known to induce the formation of nondirected dorsal filopodia in a variety of cell types, including COS-7, HEK-293, and CAD cells when overexpressed (Bohil et al., 2006), as it does in MECs in our hands (unpublished data). However, our studies indicate that most of the filopodia induced by BMP6 in MECs are substrate attached rather than dorsal projecting and unattached, yet these substrate-attached filopodial are equally dependent on Myo10 for assembly in response to appropriate cues. These observations indicate that the role of Myo10 in filopodial assembly in endothelial cells is more substantial than previous studies (Berg and Cheney, 2002; Bohil et al., 2006) suggest in that Myo10 is required for the guidance of filopodial directionality that is triggered by gradients formed by growth factors such as BMP6. It seems that directed filopodial assembly depends not only on increased levels of Myo10 but also on integration of other signals to create substrate-attached filopodia. Whether the dorsal filopodia induced by Myo10 overexpression alone represent an intermediate step in mature filopodial assembly or a terminal nonproductive architectural event remains to be determined; because β-integrin transportation by Myo10 to filopodia stabilizes filopodia by enhancing substrate attachment (Zhang et al., 2004), it seems most likely that dorsal filopodia represent an intermediate state in physiologic filopodial formation that may depend on integrin-dependent adhesive events for complete maturation to substrate attachment.

Myo10 contains an N-terminal motor domain, and the tail domains contain pleckstrin homology, MyTH4, and FERM motifs that are speculated to be the docking platform for its cargoes, such as the β-integrins that bind to the FERM motif of Myo10 (Zhang et al., 2004). Our experiments support the addition of ALK6 to the list of Myo10 cargoes based on their colocalization and the translocation of ALK6 from cytoplasmic regions into filopodia along with Myo10 (Video 1). Notably, these observations are reminiscent of the report in *Drosophila* that the Decapentaplegic receptor Thickveins is present in discrete bodies that move along filopodia-like cytonemes (Hsiung et al., 2005). Although the primary localization of Myo10 is at the tips of filopodia, puncta of Myo10 proteins are also visualized along the filopodia and in the cell body (Figs. 2 H and 6 B).

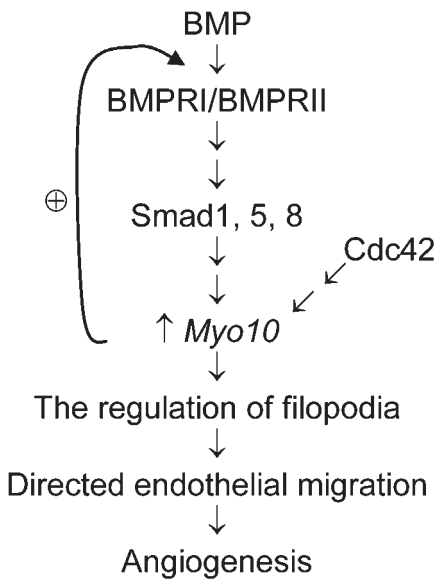

Figure 8. **Schematic model for Myo10 as a sensor for filopodia to sense the BMP6 gradient for directed cell migration and angiogenesis.**

Expression of Myo10 within the cytoplasm may indicate that pools of the protein are available for mobilization when filopodial assembly is mandated by local cues. The mean rate of the forward movements for puncta of GFP-ALK6 was $\sim 42 \pm 16$ nm s^{-1} (Fig. 6 A), which is similar to the rates of the forward movements for GFP-Myo10 (84 ± 36 nm s^{-1}) reported previously (Berg and Cheney, 2002). The data that Myo10 and ALK6 move together within the filopodia under certain circumstances further support the critical role of Myo10 in the regulation of ALK6-transduced endothelial activation (Video 2). It raises the possibility that receptors for other growth factors also may use the Myo10 machinery to regulate the function of filopodia for the perception of environmental cues.

There are two possible nonexclusive purposes for the association of ALK6 with Myo10: these interactions may be required for filopodial assembly and function, and, additionally, they may be required specifically for proper BMP signaling. In support of the former role, ALK6-deficient mice have defects in axonal path finding, which is analogous to the guidance and migration of endothelial cells (Liu et al., 2003). In addition, we have observed that confocal images of GFP-ALK6–overexpressing endothelial cells demonstrate increased filopodial assembly (unpublished data). In support of a specific role for Myo10–ALK6 interactions in the regulation of BMP signaling, we observed that the association of ALK6 and Myo10 is required for maximal BMP responses, indicating that Myo10 participates in an amplification loop for BMP signaling (Figs. 7 and 8). Conceptually, this suggests that initial activation of BMP signaling in endothelial cells provokes the cell to up-regulate Myo10, initiating filopodial assembly and BMP receptor transport to probe for additional BMP signaling cues.

Based on the results of the experiments here, we propose a model to explain how Myo10 induced by BMP6 contributes to BMP6-induced angiogenesis (Fig. 8). The activation of the BMP signaling pathway in endothelial cells leads to transcriptional activation of Myo10 expression, which, in turn, increases the formation of filopodia. Cell polarization ensues, provoking the initial steps in directed endothelial cell migration. As the BMP receptor ALK6 is translocated into filopodia by Myo10, further increases in BMP signaling occur, providing positive feedback and a second level of control for endothelial cell activation. It is noteworthy that VEGF controls sprouting angiogenesis in the early postnatal retina by guiding filopodial extensions of endothelial tip cells (Gerhardt et al., 2003). Collectively, these observations and results of the present studies indicate that filopodia may be a point of convergence for signaling pathways within endothelia and that maintenance of filopodial integrity is a crucial determinant of the guidance of endothelial migration and angiogenesis.

Materials and methods

Reagents

Mouse Myo10 cDNA was cloned into EGFP-C1 Vector (Clontech Laboratories, Inc.). ALK6 cDNA was provided by L. Attisano (University of Toronto, Toronto, Canada). Recombinant human BMP2, BMP6 protein, and anti-ALK6 antibody were obtained from R&D Systems. Anti-pSmad1, 5, and 8 antibody and anti-Smad antibody were purchased from Cell Signaling Technology. Chicken anti-Myo10 polyclonal antibody was generated against the coiled-coil region of mouse Myo10 protein (Sousa et al., 2006).

Cell culture and transfection

MECs were grown in DME supplemented with 10% FBS and antibiotics (100 U/ml penicillin and 68.6 mol/L streptomycin). The cells were cultured on glass coverslips precoated with 50 μg/ml collagen (Roche). For transient expression experiments, ~50–70% confluent MECs in 35-mm dishes were transfected 24 h after plating with 2 μg plasmids using 3 μl Lipofectamine and 3 μl Plus reagent (Invitrogen) in DME without FBS and antibiotics. After 3 h of incubation, an equal volume of DME containing 20% FBS was added to the medium. 3 h later, the media were replaced with complete DME containing 10% FBS and antibiotics. 1 d later, cells were serum starved overnight and treated with BMP6.

Construction of siRNA

Sequences 1–4 for siRNA1–4, respectively, were chosen by Dharmacon software. Myo10 siRNA1 primers (5′-GATCCGCCGTATGGCTCAACTTCGATTCAAGAGATCGAAGTTGAGCCATACGGCTTTTTTAAGCTTG-3′ and 5′-AATTCAAGCTTAAAAAAGCCGTATGGCTCAACTTCGATCTCTTGAATCGAAGTTGAGCCATATGGCG-3′) and siRNA2 primers (5′-GATCCGACCTTTGGCTCTTCAGAGATTCAAGAGATCTCTGAAGAGCCAAAGGTCTTTTTTAAGCTTG-3′ and 5′-AATTCAAGCTTAAAAAAGACCT TTGGCTCTTCGAGAGTCTCTTGAATCTCTGAAGAG-3′) were used for synthesis of double-stranded DNA (Invitrogen). The double-stranded DNA was ligated into linearized RNAi-Ready pSIREN-RetroQ-zsGreen vector (Clontech Laboratories, Inc.) for producing siRNA in transfected cells. The target sequence of the control siRNA was the DNA sequence GATCCGTGCGTTGCTAGTACCAACTTCAAGAGATTTTTTCGCGTG.

Microarray analysis

Total RNAs extracted from MECs treated with BMP2 or BMP6 for 4 h or from mock-treated controls were processed for microarray analysis (Ren et al., 2007). Cluster analysis and visualization using Java-TreeView were accomplished as previously described (Ren et al., 2007). Selected genes were validated by RT-PCR. The complete MIAME-compliant dataset is available at the Gene Expression Omnibus (http://www.ncbi.nlm.nih.gov/projects/geo/query/acc.cgi; search GSE4909).

Immunoprecipitation and Western blotting analysis

Cells were harvested in lysis buffer (1% Triton X-100, 50 mM Tris, pH 7.4, 150 mM NaCl, 1 mM Na_3VO_4, and 0.1% protease inhibitor mixture; Sigma-Aldrich) and clarified by centrifugation at 16,000 *g*. Equal amounts of proteins were incubated with a specific antibody overnight at 4°C with gentle rotation. Protein A/G Plus agarose beads (Santa Cruz Biotechnology, Inc.) were used to pull down the antibody complexes. Afterward, beads were washed with lysis buffer, and immune complexes were separated

by SDS-PAGE. Total cell lysates were separated by SDS-PAGE and transferred to nitrocellulose membranes.

Immunofluorescence

Cells were fixed in 3.7% PFA for 10 min at room temperature. After three washes with PBS, the cells were sequentially treated with 0.2% Triton X-100 for 5 min (for permeabilization), with 5% boiled serum for 1 h (for blocking), and then with the primary antibody overnight in the blocking solution. After three washes, cells were incubated in the dark with second antibody and/or phalloidin conjugated with AlexaFluor488 or 594 (Invitrogen) in blocking solution for 90 min at 37°C. After three washes in PBS, the cells were counterstained with DAPI, and the fluorescent signal was visualized by a fluorescence microscope or confocal laser-scanning microscope (LSM5 Pascal; Carl Zeiss, Inc.).

SEM experiments

The experiments were performed as previously described (Bohil et al., 2006). Cells grown on coverslips were rinsed briefly with PBS, prefixed with 3.7% PFA for 5 min, and rinsed three times with PBS. To identify and record the positions of individual transfected cells, the coverslips were imaged with fluorescence by using an inverted microscope (DMIRB; Leica) and a 10× 0.75 NA dry lens. Coverslips were then prepared for SEM by using standard procedures, SEM images of the transfected cells were taken, and filopodia were counted. Filopodia were defined as thin (<1 μm wide) protrusions that extended at least 0.75 μm from the cell margin.

Dunn chamber assay

MECs were seeded on 50 μg/ml collagen–coated coverslips and starved for 18 h before assay. To set up gradient experiments, both concentric wells of the chamber were filled with starvation medium (DME with 1% FBS), and a coverslip seeded with cells was inverted onto the chamber in an offset position, leaving a narrow slit at one edge for refilling the outer well. The coverslip was sealed in place using hot wax mixture around all of the edges except for the filling slit. The medium of the outer well was drained and replaced with medium containing 1% FBS and 200 ng/ml BMP6. The slit was then sealed with hot wax mixture. For control experiments in which cells were subjected to uniform concentrations of chemoattractant, both wells were filled with medium containing 0 or 200 ng/ml BMP6. At the end of each migration assay, guidemarks were drawn on the coverslip to mark the limits of the Dunn chamber annular bridge. All of the cells within the annular bridge were processed for confocal microscopy analysis (LSM5 Pascal; Carl Zeiss, Inc.) with a 63× oil objective (Carl Zeiss, Inc.). The cells within the inner well and outer well served as internal controls.

Boyden chamber assay

Boyden chamber assay was performed as previously described (Ren et al., 2007). The Boyden chamber is a 48-well chamber apparatus (NeuroProbe). The lower chambers of the apparatus were filled with DME with or without BMP6 and were covered with the collagen-coated filter and the upper chambers. Cells pretreated with or without BMP6 were then added to the upper chambers. After incubating for 6 h at 37°C, cells present on the lower surface were fixed, stained, and identified with the 40× objective lens on an inverted microscope (Eclipse TS100; Nikon).

Wound-healing assay

For detection of cell migration, a wound-healing assay was performed as previously described (Pi et al., 2005). MECs were grown on 35-mm wells, the monolayer was scratched with a sterile disposable rubber policeman, and the edge was labeled with a traced line. After injury, the cells were gently washed with normal medium without serum. Endothelial cell migration from the edge of the injured monolayer was quantified by measuring the area between the wound edges before and the recovered area after injury using light microscopy (Eclipse TS100; Nikon), a 4× objective, and the computer program ImageJ (National Institutes of Health).

In vitro matrigel angiogenesis assay

Endothelial cell tube formation was analyzed with the matrigel-based tube formation assay (Pi et al., 2005; Ren et al., 2007). Chilled 24-well plates were coated with growth factor–reduced matrigel (Becton Dickinson) that was polymerized at 37°C for 30 min. MECs were transfected with siRNA constructs with Lipofectamine-Plus reagents. The next day, cells were serum starved for 1 h, trypsinized, and plated at equal numbers into each matrigel-coated well. After 6 h of incubation in the absence or presence of BMP6, the formation of tubes was photographed with a camera (Eclipse TS100; Nikon) and a 10× objective. Images were quantified with ImageJ.

Angiogenesis assay in 3D collagen gel

A solution of rat type I collagen was prepared by mixing collagen solution with 5× PBS and neutralization buffer in distilled water according to the manufacturer's suggestion (Chemicon). MECs suspended in DME were diluted in the collagen gel to a final density of 2×105 cells ml^{-1}. To form the gel, 0.5 ml of the MEC/collagen mixture was plated per well in an uncoated 24-well plate. BMP6 was added to the MEC/collagen mixture before collagen polymerization. After the collagen was allowed to polymerize for 20 min at 37°C, the gels were overlaid with 0.5 ml DME supplemented with BMP6 or control. Tube formation was observed at 24 h and analyzed with ImageJ.

Statistical analysis

Data were shown as mean ± SD for three to four separate experiments. Differences were analyzed with a *t* test. Values of $P < 0.05$ were considered statistically significant.

Online supplemental material

Video 1 shows live cell imaging of GFP-tagged ALK6 translocating from cell body to filopodia in an MEC treated with BMP6 for 4 h. Video 2 shows live cell imaging of the movement of GFP-tagged Myo10 and RFP-tagged ALK6 in the filopodia of MECs. Fig. S1 shows how Myo10 knockdown with siRNA inhibits BMP6-directed migration of MECs pretreated with BMP6 and VEGF but not with SIP or FGF-2. Fig. S2 shows how Myo10 knockdown with siRNA inhibits BMP6-induced random migration in endothelial cells. Fig. S3 shows micrographs highlighting structural details associated with tube formation by MECs cultured in collagen gel in the presence of BMP6 treatment. Table S1 presents data on endothelial random migration parameters after BMP6 treatment. Online supplemental material is available at http://www.jcb.org/cgi/content/full/jcb.200704010/DC1.

We thank Robert Bagnell, Victoria J. Madden, and Elena Davis for assistance with SEM, confocal microscopy, and real-time cell imaging experiments.

This work was supported by National Institutes of Health grants HL 61656, HL 03658, and HL 072347 to C. Patterson and a postdoctoral fellowship from the American Heart Association to X. Pi. It was also supported by National Institutes of Health grant HL080166 to R.E. Cheney and a predoctoral fellowship from the American Heart Association to A.B. Bohil. C. Patterson is an Established Investigator of the American Heart Association and a Burroughs Wellcome Fund Clinician Scientist in Translational Research.

Submitted: 2 April 2007
Accepted: 24 November 2007

References

Bar, T., and J.R. Wolff. 1972. The formation of capillary basement membranes during internal vascularization of the rat's cerebral cortex. *Z. Zellforsch. Mikrosk. Anat.* 133:231–248.

Berg, J.S., and R.E. Cheney. 2002. Myosin-X is an unconventional myosin that undergoes intrafilopodial motility. *Nat. Cell Biol.* 4:246–250.

Bohil, A.B., B.W. Robertson, and R.E. Cheney. 2006. Myosin-X is a molecular motor that functions in filopodia formation. *Proc. Natl. Acad. Sci. USA.* 103:12411–12416.

Deckers, M.M., R.L. van Bezooijen, G. van der Horst, J. Hoogendam, C. van Der Bent, S.E. Papapoulos, and C.W. Lowik. 2002. Bone morphogenetic proteins stimulate angiogenesis through osteoblast-derived vascular endothelial growth factor A. *Endocrinology.* 143:1545–1553.

Folkman, J., and M. Klagsbrun. 1987. Vascular physiology. A family of angiogenic peptides. *Nature.* 329:671–672.

Gerhardt, H., M. Golding, M. Fruttiger, C. Ruhrberg, A. Lundkvist, A. Abramsson, M. Jeltsch, C. Mitchell, K. Alitalo, D. Shima, and C. Betsholtz. 2003. VEGF guides angiogenic sprouting utilizing endothelial tip cell filopodia. *J. Cell Biol.* 161:1163–1177.

Hogan, B.L. 1996. Bone morphogenetic proteins in development. *Curr. Opin. Genet. Dev.* 6:432–438.

Hsiung, F., F.A. Ramirez-Weber, D.D. Iwaki, and T.B. Kornberg. 2005. Dependence of *Drosophila* wing imaginal disc cytonemes on Decapentaplegic. *Nature.* 437:560–563.

Klagsbrun, M., and P.A. D'Amore. 1991. Regulators of angiogenesis. *Annu. Rev. Physiol.* 53:217–239.

Klosovskii, B.N., and T.P. Zhukova. 1963. Effect of colchicine on remote phases of growing capillaries in the brain. *Arkh. Patol.* 35:38–44

Liu, J., S. Wilson, and T. Reh. 2003. BMP receptor 1b is required for axon guidance and cell survival in the developing retina. *Dev. Biol.* 256:34–48.

Marin-Padilla, M. 1985. Early vascularization of the embryonic cerebral cortex: Golgi and electron microscopic studies. *J. Comp. Neurol.* 241:237–249.

Massague, J. 1998. TGF-beta signal transduction. *Annu. Rev. Biochem.* 67:753–791.

Moutsatsos, I.K., G. Turgeman, S. Zhou, B.G. Kurkalli, G. Pelled, L. Tzur, P. Kelley, N. Stumm, S. Mi, R. Muller, et al. 2001. Exogenously regulated stem cell-mediated gene therapy for bone regeneration. *Mol. Ther.* 3:449–461.

Patan, S. 2000. Vasculogenesis and angiogenesis as mechanisms of vascular network formation, growth and remodeling. *J. Neurooncol.* 50:1–15.

Patan, S., L.L. Munn, and R.K. Jain. 1996. Intussusceptive microvascular growth in a human colon adenocarcinoma xenograft: a novel mechanism of tumor angiogenesis. *Microvasc. Res.* 51:260–272.

Pi, X., G. Garin, L. Xie, Q. Zheng, H. Wei, J. Abe, C. Yan, and B.C. Berk. 2005. BMK1/ERK5 is a novel regulator of angiogenesis by destabilizing hypoxia inducible factor 1alpha. *Circ. Res.* 96:1145–1151.

Raida, M., J.H. Clement, R.D. Leek, K. Ameri, R. Bicknell, D. Niederwieser, and A.L. Harris. 2005. Bone morphogenetic protein 2 (BMP-2) and induction of tumor angiogenesis. *J. Cancer Res. Clin. Oncol.* 131:741–750.

Ren, R., P.C. Charles, C. Zhang, Y. Wu, H. Wang, and C. Patterson. 2007. Gene expression profiles identify a role for cyclooxygenase 2-dependent prostanoid generation in BMP6-induced angiogenic responses. *Blood.* 109:2847–2853.

Small, J.V. 1988. The actin cytoskeleton. *Electron Microsc. Rev.* 1:155–174.

Sousa, A.D., and R.E. Cheney. 2005. Myosin-X: a molecular motor at the cell's fingertips. *Trends Cell Biol.* 15:533–539.

Sousa, A.D., J.S. Berg, B.W. Robertson, R.B. Meeker, and R.E. Cheney. 2006. Myo10 in brain: developmental regulation, identification of a headless isoform and dynamics in neurons. *J. Cell Sci.* 119:184–194.

ten Dijke, P., O. Korchynskyi, G. Valdimarsdottir, and M.J. Goumans. 2003. Controlling cell fate by bone morphogenetic protein receptors. *Mol. Cell. Endocrinol.* 211:105–113.

Tessier-Lavigne, M., and C.S. Goodman. 1996. The molecular biology of axon guidance. *Science*. 274:1123–1133.

Valdimarsdottir, G., M.J. Goumans, A. Rosendahl, M. Brugman, S. Itoh, F. Lebrin, P. Sideras, and P. ten Dijke. 2002. Stimulation of Id1 expression by bone morphogenetic protein is sufficient and necessary for bone morphogenetic protein-induced activation of endothelial cells. *Circulation*. 106:2263–2270.

Wozney, J.M. 2002. Overview of bone morphogenetic proteins. *Spine*. 27:S2–S8.

Yamashita, H., A. Shimizu, M. Kato, H. Nishitoh, H. Ichijo, A. Hanyu, I. Morita, M. Kimura, F. Makishima, and K. Miyazono. 1997. Growth/differentiation factor-5 induces angiogenesis in vivo. *Exp. Cell Res.* 235:218–226.

Yang, X., L.H. Castilla, X. Xu, C. Li, J. Gotay, M. Weinstein, P.P. Liu, and C.X. Deng. 1999. Angiogenesis defects and mesenchymal apoptosis in mice lacking SMAD5. *Development*. 126:1571–1580.

Zhang, H., and A. Bradley. 1996. Mice deficient for BMP2 are nonviable and have defects in amnion/chorion and cardiac development. *Development*. 122:2977–2986.

Zhang, H., J.S. Berg, Z. Li, Y. Wang, P. Lang, A.D. Sousa, A. Bhaskar, R.E. Cheney, and S. Stromblad. 2004. Myosin-X provides a motor-based link between integrins and the cytoskeleton. *Nat. Cell Biol.* 6:523–531.

Zicha, D., G.A. Dunn, and A.F. Brown. 1991. A new direct-viewing chemotaxis chamber. *J. Cell Sci.* 99:769–775.